Made available by Hasselt University Library in https://documentserver.uhasselt.be

Short-term phytotoxicity in Brassica napus (L.) in response to pre-emergently applied metazachlor: A microcosm study

Peer-reviewed author version

VERCAMPT, Hanne; Koleva, Lyubka; Vassilev, Andon; VANGRONSVELD, Jaco & CUYPERS, Ann (2017) Short-term phytotoxicity in Brassica napus (L.) in response to pre-emergently applied metazachlor: A microcosm study. In: ENVIRONMENTAL TOXICOLOGY AND CHEMISTRY, 36(1), p. 59-70.

DOI: 10.1002/etc.3538
Handle: http://hdl.handle.net/1942/23281

Running head:

Short-term phytotoxic effects of metazachlor on oilseed rape

Corresponding author:

Cuypers Ann

Agoralaan Building D, 3590 Diepenbeek, Belgium

Tel +32 11 268326

E-mail ann.cuypers@uhasselt.be

Title:

Short-term phytotoxicity in *Brassica napus* (L.) in response to pre-emergently applied metazachlor: a microcosm study

Vercampt Hanne[†], Koleva Lyubka[‡], Vassilev Andon[‡], Vangronsveld Jaco[†] and Cuypers Ann[†]*

[†]Hasselt University, Centre for Environmental Sciences, Agoralaan Building D, 3590 Diepenbeek, Belgium

[‡]Agricultural University of Plovdiv, Department of Plant Physiology and Biochemistry, Plovdiv, Bulgaria

*Corresponding author: **E-mail** ann.cuypers@uhasselt.be **Tel** +32 11 268326

ABSTRACT

In accordance with realistic application approaches, a short-term one-factorial experiment was set up to investigate the phytotoxic impact of pre-emergent application of the chloroacetamide herbicide metazachlor on *Brassica napus*. In addition to morphological parameters, the underlying processes that ultimately determine the extent of herbicide-induced phytotoxicity, *i.e.* herbicide metabolisation and cellular antioxidant defence, were examined. The present study demonstrated that metazachlor provoked fasciation of the leaves closely after emergence, which could possibly be addressed to its working mechanism whereby cell division is impaired through the inhibition of very long chain fatty acid synthesis. The increased activities of antioxidative enzymes and metabolites in leaf tissue indicated the presence of reactive oxygen species under the influence of metazachlor. This resulted in oxidative damage in the form of membrane lipid peroxidation. Simultaneously, the increased activity of glutathione-S-transferase (GST) and the shift in glutathione (GSH) redox state suggested the activation of the detoxification metabolism. This occurred however at the expense of growth, with a temporary reduction in plant height and weight after application. The results indicated that metazachlor disappeared within 3 to 4 months after application, which resulted in the recovery of the crop. In conclusion, metazachlor induces phytotoxicity in the short-term, either directly through its mode of action or indirectly through the induction of oxidative stress, which resulted in a temporary reduction in growth.

Key words: *Brassica napus*, metazachlor, phytotoxicity, stress response, toxic effects

INTRODUCTION

Metazachlor is a pre-emergently used herbicide in the cultivation of the oilseed crop, *Brassica napus*, to chemically prevent the settling and growth of broadleaved weeds and annual grasses. As a chloroacetamide, metazachlor is known for inhibiting lipid biosynthesis and hence the formation of very long chain fatty acids (VLCFA) [1]. Like most herbicides, metazachlor can affect other non-target species via soil infiltration, drainage and run-off [2,3]. Even before it enters the ecosystem, the herbicidal compound can potentially affect the cultivated crop. This can subsequently result in reductions in yield [4], morphological aberrations [5], induction of oxidative stress [6], increased lipid peroxidation of membranes [7] and decreased chlorophyll content [8]. Results derived from field experiments are often subject to large variations between plots from a certain condition, resulting in a lack of statistical support. This is due to the fact that field experiments cannot exclude the complex interaction of external factors, such as direction and rate of drainage, the presence of herbivores (*e.g.* snails), heterogeneity of the soil, etc. This microcosm study aims to exclude these side effects by the use of a one-factorial experimental set-up.

The occurrence and extent of phytotoxicity of metazachlor in *B. napus* are determined either by the crop's capacity to detoxify the herbicide or its capacity to cope with metazachlor-induced oxidative stress. The detoxification metabolism of a crop plays an important role in the tolerance of a crop against herbicides, with a significant role for glutathione-S-transferase (GST) [9,10]. Once herbicidal compounds are present in the cell cytoplasm the structure and reactivity of the compound will be modified by cytochrome P450 proteins in the first phase of detoxification. In the second phase, the modified herbicidal compound is conjugated with glutathione (GSH) by the action of GSTs. In the third phase of herbicide detoxification, GSH will function as a tag for the compartmentalization of the herbicidal compound into either the vacuole or the cell membrane. Herbicidal compounds are

known to induce the activity of GST in most crops species [6,11,12]. Based on their sequence identity, gene organisation and active site residues, plant GST's can be divided into 5 classes; tau, phi, theta, zeta and lambda [13]. Tau and phi class GSTs are plant-specific and do not occur in mammalian species like all other plant GST classes. GST isoenzymes that belong to the same class have a 40 to 60 % identity in their primary structure. Structurally, GSTs are composed of 2 subunits that can be either identical (homodimeric) or distinct (heterodimeric). Each subunit contains a kinetically independent active site with distinct domains for the GSH (G-site) and the electrophilic substrate (H-site). With each subunit encoded by a separate gene, plants contain complex multigene families of GSTs. Hence, the various subunits may be able to dimerise in many permutations, producing multiple homo- and hetero-dimeric GST isoenzymes [14]. The GST isoenzymes involved in xenobiotic metabolism are subjected to discrete regulation, showing distinct but overlapping substrate specificities. From complementation studies, it is likely that quite dissimilar GSTs share similar functions [15]. Despite the association between GSTs and plant stress responses, it remains unclear whether different GST classes are substrate specific. The inducibility of phi and tau class GSTs after plant exposure to either biotic or abiotic stresses is a characteristic feature of these genes [16]. Several tau class GSTs are known to be strongly induced during cell division [16]. Phi class GSTs have been shown to be highly reactive towards chloroacetamide and thiocarbamate herbicides [11,17].

Initially after herbicide application, when detoxification is either activated or at its full turnover, the non-detoxified fraction of cytosolic herbicidal compounds can indirectly cause oxidative damage at different cellular levels by the induction of oxidative stress. Herbicide-induced oxidative stress has been described in crops [18,19] and for chloroacetamides, such as alachlor and metolachlor, in particular [20,21]. Herbicides from different classes of mode of action can negatively affect crop morphology [22] and physiology, ranging from

92 destabilisation of cellular membranes [23] to pigment profiles [24]. However, the underlying
93 mechanisms of phytotoxicity are not well addressed in literature. Due to the relatively short
94 degradation rate of metazachlor, which ranges between 3 to 4 months, it is important to
95 monitor metazachlor-induced phytotoxicity closely after application in this short-term
96 microcosm study. A one-factorial microcosm experiment was set up to monitor (i) growth,
97 development and herbicide uptake of the crop *B. napus* during 9 weeks after treatment with
98 metazachlor and (ii) to monitor cellular structure, such as membrane integrity, pigment and
99 nutrient content, and cell functioning, such as herbicide detoxification and antioxidant
100 defence mechanism, of *B. napus* within 2 and 4 weeks after pre-emergent application of
101 metazachlor.

MATERIALS AND METHODS

Experimental design and methodology

Three days before sowing, *B. napus* (cultivar *Remy*) seeds were surface sterilised. Hereby, seeds were washed in a 0.1 % sodium hypochlorite solution for 2 min and subsequently rinsed thoroughly with deionised water. Next, seeds were rinsed in deionised water for 20 min and then stored in a closed Petri dish on a moistened filter. After being incubated in the dark at 4 °C during 2 nights, seeds were separately sown in microcosms on 1.3 kg sandy soil at approximately 1 cm depth. In each microcosm 6 seeds were sown. The day after sowing, 10 mL of metazachlor solution was applied on the soil surface in the following concentrations; 0 mM, 0.2 mM and 0.4 mM metazachlor, which corresponded with 0 mg, 0.5 mg and 1 mg active ingredient per microcosm. Every 2 days, 10 to 50 mL ½ Hoagland nutrient solution was supplied. Plants were grown in a growth chamber under controlled environmental conditions set at a 12 h photoperiod, 65 % relative humidity and day/night temperatures of 22 °C and 18 °C, respectively. A combination of blue, red and far-red LED modules simulated the photosynthetic active radiation (PAR) of 200 µmol /m^2s of sunlight. Germination was determined by counting the percentage of seeds emerged within 7 days after metazachlor application. Thereafter, the amount of plants was reduced to 1 plant per microcosm. Growth was monitored daily during 7 weeks by determining the growth stage of each individual plant according to Lancashire et al. [25]. Metazachlor uptake into the aboveground plant parts was monitored 14, 28 and 42 days after treatment (DAT). Leaf tissue for biochemical analyses was collected 14 and 28 DAT, snap frozen in liquid nitrogen and subsequently stored at -70 °C. During sampling, weight, root and shoot length were measured. In addition to these time points, fresh weight was recorded at 9 weeks after treatment (63 DAT).

Lipid peroxidation

Lipid peroxidation of cell membranes was determined by the measurement of thiobarbituric acid (TBA) reactive metabolites [26]. Fresh leaf tissue (100 mg) was homogenised in 0.1 % trichloroacetic acid (TCA). After 30 min of incubation with 0.5 % TBA in 20 % TCA at 95 °C, the extract was cooled for 5 min on ice (4 °C) and subsequently centrifuged for 10 min at 20.000 g (4 °C). The absorbance of the supernatant was measured at 532 nm and corrected for unspecific binding at 600 nm.

Pigment profile

Chlorophyll *a*, chlorophyll *b* and carotenoid concentrations were determined according to Lichtenthaler et al. [27]. Fresh leaf material (100 mg) was homogenised in 80 % acetone in cooled mortars, in darkness. After centrifugation (9.000 g, 5 min), the volume of the supernatant was determined and subsequently 10 times diluted in 80 % acetone. The leaf extract was measured spectrophotometrically at 663 nm, 646 nm and 470 nm, and subsequently the pigment profile was calculated.

Potassium leakage

Potassium leakage was monitored as a measure for cell membrane stability. After cutting a leaf, the surface of the leaf was washed with Milli-Q water, dried and subsequently cut in 2 halves. Thereby, the main leaf nerve was removed. After weighing each half of the leaf, one part was incubated in 10 mL of Milli-Q water at 4°C during 3 hours and the other part was incubated in10 mL of Milli-Q water at 95°C during 3 hours. The concentration of potassium was determined in both extracts by ICP-OES and represented the extracellular and the total concentration of potassium present in the leaf, respectively.

H_2O_2 quantification

The presence of H_2O_2 in the first leaf pair was determined by qualitative 3,3'-diaminobenzidine (DAB) staining [28]. As DAB precipitates as a brown complex after being oxidised by H_2O_2, the latter could be located visually. Leaves were carefully cut at their basis, put in the dark and immediately vacuum infiltrated with DAB in 10 mM Na_2HPO_4 buffer (pH 3) for 5 min. Subsequently the samples were shaken for 4 h at 80 rpm in dark conditions. After being bleached for 15 min in ethanol:acetic acid:glycerol (3:1:1) at 95 °C, leaves were stored in acetic acid (20 %) at 4 °C before being monitored. The following day, detailed close-up pictures were taken from each separate leaf using a binocular microscope, a digital camera and BTV-pro software (Bensoftware).

Total antioxidant capacity

The ferric reducing antioxidant capacity (FRAP) assay was used to determine the capacity of lipophilic and hydrophilic antioxidant fractions [29]. Fresh leaf tissue (100 mg) was homogenised in 0.01 N Na-EDTA. After centrifugation (30 min, 15.000 g, 4 °C), the hydrophilic fraction was located in the supernatant. The lipophilic fraction, which was located in the pellet, was further extracted in 80 % acetone before analysis. Freshly prepared FRAP reagent, containing 100 mM 2,4,6-Tris(2-pyridyl)-*s*-triazine (TPTZ) and 200 mM $FeCl_3$ in sodium acetic buffer (pH 3.6-4), was added to both fractions. The measurement of the anti-oxidative capacity of the sample was based on its ability to reduce the yellow-coloured Fe^{3+}-TPTZ complex to the blue-coloured ferrous form, which was spectrophotometrically recorded at 593 nm. The results were calculated by standard curves prepared with known concentrations of Trolox and were expressed as µmol Trolox equivalents/g FW.

Antioxidant enzyme activities

Proteins were extracted from leaf samples by a 2-step ammonium sulphate precipitation method. All steps were performed at 4 °C. Leaf material was incubated for 30 min in fresh 0.1 M Tris/HCl buffer (pH 7.8), containing 5 mM EDTA, 5 mM DTE, 1% PVP and 1 % Nondidet. After 30 min of centrifugation (50.000 g), the supernatant was incubated for 30 min with 40 % $(NH_4)_2\ SO_4$. After a second round of centrifugation, the supernatant was incubated for 30 min with 80 % $(NH_4)_2\ SO_4$. The extract was subsequently desalted by running over PD 10 columns (2 min, 950 g, 4 °C) and directly stored at -80 °C for further analysis of enzyme activities. All enzyme activities were determined at 25 °C in 1 mL cuvettes. Eight biological replicates were used from each condition.

Superoxide dismutase (SOD) activity was determined in 33 mM KH_2PO_4 reaction buffer (pH 7.8) and 0.1 mM EDTA [30]. By adding 60 mU xanthine oxidase to 0.05 mM xanthine, uric acid is formed. In this reaction, superoxide is formed as a by-product and reduces cytochrome C (0.01 mM) in a blank sample. By adding plant extract, SOD activity is calculated indirectly by measuring the inhibition of formation of reduced cytochrome C at 550 nm. The amount of SOD inhibiting the production of reduced Cyt C with 50 % is defined as 1 unit of SOD activity.

Catalase (CAT) activity was determined in 75 mM KH_2PO_4 reaction buffer (pH 7) [31]. After addition of 1 mM H_2O_2, catalase activity is calculated by the rate at which H_2O_2 is reduced to H_2O and O_2 and hence by measuring the decrease of H_2O_2 spectrophotometrically at 240 nm.

Glutathione reductase (GR) was determined in 1 mM Tris and 1 mM EDTA reaction buffer (pH 8) [31]. By adding 1.5 mM glutathione disulfide (GSSG) and 0.1 mM NADPH to the reaction buffer, GR present in the leaf extract catalyses the reduction of GSSG to GSH, through simultaneous consumption of NADPH. Measuring the oxidation of NADPH at 340 nm makes it possible to calculate the GR activity.

Guaiacol peroxidase (GPx) was determined in 75 mM KH_2PO_4 reaction buffer (pH 7) [31]. Adding 1 mM H_2O_2 and 2 mM guaiacol to the reaction buffer, leaf extract catalyses the conversion of H_2O_2 into H_2O and O_2 by oxidation of guaiacol, which was measured spectrophotometrically at 436 nm.

Syringaldazine peroxidase (SPx) was determined in 80 mM Tris-HCl reaction buffer (pH 7.5) [32]. Syringaldazine substrate (55 µM) was oxidised by SPx simultaneously with the reduction of 1 mM H_2O_2 and was monitored at 530 nm.

Glutathione-S-transferase (GST) activity was determined using different standard substrates: 1 mM 1-chloro-2,4-dinitrobenzene (CDNB), 1 mM 1,2-dichloro-4-nitrobenzene (DCNB), 1 mM 4-nitrobenzyl chloride (NBC), 1 mM p-nitrobenzoyl chloride (NBoC), 0.5 mM p-nitrophenylacetate (p-Npa) and fluorodifen (1.2 mM) [33,34]. By adding 1 mM glutathione (GSH) to 1 mM of substrate in 75 mM KH_2PO_4 reaction buffer (pH 6.5), the formation of conjugate was measured at respective wavelengths (340 nm, 345 nm, 310 nm, 310 nm, 400 nm and 400 nm).

Ascorbate peroxidase (APx) activity was determined after a separate extraction [35]. Plant tissue (100 mg) was extracted using a modified extraction buffer, containing 0.1 M Tris-HCl (pH 7.8), 1 mM DTT, 1 mM EDTA and 10 mM ascorbate. Ascorbate peroxidase reduces H_2O_2 by oxidation of ascorbate (AsA) into dehydroascorbate (DHA). Adding 20 mM H_2O_2 to the reaction buffer (0.1 M Hepes and 1 M EDTA, pH 7), made it possible to calculate APx activity in leaf extract by monitoring the decrease of ascorbate (AsA) at 298 nm.

Metabolite concentration and redox state

Leaf tissue was extracted in 200 mM HCl. After centrifugation (16.000 g, 10 min, 4°C), the supernatant was diluted with 200 mM NaH_2PO_4 (pH 5.6) and brought to pH 4.5 by addition of 200 mM NaOH. This extract was used for determination of both AsA and GSH

concentrations and their redox state [36]. Eight biological replicates were used from each condition. Ascorbate determination was based on ascorbate oxidase (AO) mediated oxidation of AsA. Dithiotreitol (DTT, 25 mM) was added to one half of the leaf extract, reducing all present DHA. By addition of AO to the subsample without DTT and the subsample with DTT, the reduced fraction (AsA) and the total fraction of ascorbate (AsA & DHA) could be determined by spectrophotometric measurement of the decrease in reduced ascorbate at 265 nm. Glutathione measurement was based on GSH mediated reduction of 5,5'-dithiobis-2-nitrobenzoic acid (DTNB) that was analysed using a spectrophotometer at 412 nm. By incubating half of the plant extract with 2-vinylpiridine for 30 minutes at 20°C, GSH was inactivated and only the present oxidised fraction of glutathione (GSSG) could be measured. By addition of GR to both incubated and non-incubated subsamples, GSSG and total GSH concentration could be determined by monitoring the reduction of DTNB by GSH.

Metazachlor determination in leaves

Metazachlor was determined in aboveground biomass via reverse-phased high performance liquid chromatography (RP-HPLC) (Adept CE-4200, Dual Piston Pump CE 4120, UV/VIS detector and Power Stream software, United Kingdom). For extraction, 5 g of fresh plant tissue was homogenized in 5 mL pure acetonitrile (HPLC grade JTBaker ®). To improve the recovery of polar components and to facilitate the partitioning of the solvent, 2 g $MgSO_4$ was added to the extract. In order to reduce the amount of polar interferences 0.5 g NaCl was added. By the addition of 0.5 g Na_3 Citrate x 2 H_2O and 0.25 g Na_2H Citrate x 1.5 H_2O, the optimal pH of 6.5 was maintained. The extract was centrifuged for 5 min at 1057 g at room temperature. One mL of supernatant was transferred to a dispersive centrifuge tube (Spectrum ®, Chemical MFG Corp.) containing 25 mg of primary secondary amine and 150 mg $MgSO_4$ and 2.5 mg of graphitised carbon black to remove

pigments. The tubes were mixed for 30 s and then centrifuged again for 5 min at 1057 g. Subsequently, the collected supernatant was analysed by RP-HPLC. The samples were analysed at 220 nm in a gradient regime by an analytical column Supelcosil LC-18 150 x 4.6 mm, 5 µm. The injected volume was 20 µL. The mobile phase composition was: phase A acetonitrile: water (40:60) and phase B acetonitrile: water (80:20). The gradient was applied for 20 min in the following regime; 0 min - 100 % A: 0 % B, 10 min - 50 % A: 50 % B, 20 min - 0 % A: 100 % B, with a flow rate of 1 mL/min. The limit of quantification and the limit of detection of this analytical method contained 1.1 µg/mL and 0.4 µg/mL, respectively. Quantification was based on a metazachlor standard curve prepared with certified metazachlor standard (98.5 %, Dr Ehrenstorfer GmbH).

Nutrient profile in leaves

Dry leaf material (0.1-0.5 g) was digested in 70-71 % HNO_3 and dissolved in 2 % HCl. After digestion, the clear colourless extract was brought to 25 mL volume with Milli-Q water. Macronutrients (P, K, Mg, Ca, S) and micronutrients (Na, Fe, Cu, Zn, Mn) present in plant extracts were determined by inductively coupled plasma – optical emission spectroscopy (ICP-OES 710, Agilent Technologies, Australia). Concentrations were calculated by the use of standard curves with known concentrations.

Statistical analyses

All data were processed according to one-way or 2-way ANOVA tests in open-source R software (R 3.1.2, The R Foundation for Statistical Computing, Vienna, Austria), in strict accordance to parametrical conditions. Normal distribution of the data was tested using Shapiro-Wilk test. Following the ANOVA, post-hoc Tukey test was performed for multiple pairwise comparisons. In case parametrical conditions were not met, Kruskall-Wallis,

277 followed by 2-by-2 Wilcoxon post-hoc comparison analyses were performed. Data are
278 represented as mean values ± standard error (SE) and significance was set at 5 % level.
279

RESULTS

Growth, development and morphology of B. napus

Seven days after metazachlor application, seed germination was 10 % lower in microcosms treated with 0.2 and 0.4 mM metazachlor in comparison to the non-treated microcosms, although not significant (data not shown). Two weeks after treatment (14 DAT) 1.12 and 1.58 mg metazachlor /kg FW were found in the aerial parts of 0.2 and 0.4 mM metazachlor-treated plants, respectively. During the following 4 weeks, the levels of metazachlor decreased with 78 % and 64 % in the aerial plant parts of the respective treatments to 0.24 and 0.57 mg metazachlor /kg FW (42 DAT) (Figure 1). Closely after application leaves displayed fasciation in the form of crinkled leaves, shortened mid ribs and incomplete detachment of the leaves under the influence of metazachlor (Figure 2). These malformations appeared within the first 2 to 6 weeks after treatment and remained present until leaves' abscission during further development. Twenty-one DAT 20 % and 50 % of the plants treated with 0.2 and 0.4 mM metazachlor, respectively, displayed signs of fasciation and 20 % of the plants in both treatments did not survive the first 7 weeks (data not shown). Weight and height were strongly inhibited in 0.2 and 0.4 mM metazachlor-exposed plants at 14 DAT in a dose dependent way (Figure 3A, Figure 4 and Table 1). Twenty-eight DAT, these differences still existed (Figure 3B and Table 2), but at 63 DAT fresh weights of plants under different exposures were equal (Figure 3C). When taking a closer look into the rate of development of leaves of the young seedlings, no apparent differences were observed up to 5 weeks after metazachlor application (35 DAT) (Figure 5). However, considering leaf surface area and petiole length, the leaves appeared to be smaller under the influence of metazachlor, with smaller leaf surface area and shorter petioles which might explain the reduction in aboveground weight in the short term (Supplemental data S1). Between 5 and 7 weeks after application, metazachlor-exposed plants tended to develop leaves faster than control plants.

At 47 DAT, for example 30 % and 70 % of 0.2 and 0.4 mM metazachlor-exposed plants respectively, were situated in growth stage 19 or 20, meaning that these plants had developed 9 or more leaves whereas all control plants had developed maximal 8 leaves (Figure 5).

Enzymes and metabolites involved in detoxification

The activity of GST significantly increased under the influence of metazachlor, at 14 and 28 DAT (Tables 1 and 2, Figure 6). The activity of GST was increased towards chlorodinitrobenzene (CDNB), fluorodifen and nitrophenylacetate (Npa) substrates and not found for 1,2-dichloro-4-nitrobenzene (DCNB), 4-nitrobenzyl chloride (NBC) and p-nitrobenzpyl chloride (NBoC), with the strongest induction towards CDNB (Tables 1 and 2). At both time points, the level of GSH, which is consumed during GST-catalysed metabolisation of xenobiotics such as herbicides, tended to be lower under the influence of metazachlor (Figure 6). Whereas this trend could not be statistically underpinned, the redox state of glutathione was significantly turned towards the oxidised form (GSSG) at 14 DAT under influence of 0.4 mM metazachlor (Table 1). At 28 DAT, the redox state of GSH was similar in all treatments.

Metazachlor induces oxidative stress in the leaves of B. napus

The presence of reactive oxygen species (ROS), *e.g.* H_2O_2, was visualised using 3,3'-diaminobenzidine staining. No differences in the presence of H_2O_2 were detected at 14 DAT since DAB staining was restricted to the veins in all conditions (Supplemental data S2). At 14 DAT, the total antioxidative capacity (TAC) in the leaves of *B. napus* tended to increase under the influence of metazachlor, however this trend could not be statistically supported (Table 1). At 28 DAT, a significant increase in the lipophilic fraction of antioxidants was observed (Table 2). Additionally, the activities of enzymes involved in the antioxidative

defence (SOD, CAT, APx and GR) and cell wall lignification (GPx and SPx) were measured. In general, the activities of all antioxidative enzymes increased with exposure to increasing metazachlor doses (Tables 1 and 2). A higher activity in metazachlor-treated plants in comparison to non-treated plants could be statistically confirmed for catalase (CAT), ascorbate peroxidase (APx) and syringaldazine peroxidase (SPx) at 14 DAT and for superoxide dismutase (SOD), catalase (CAT), glutathione reductase (GR) and guaiacol peroxidase (GPx) at 28 DAT. Twenty-eight DAT, the levels of AsA were not affected by the applied metazachlor treatments. Together with AsA, GSH is a key metabolite in the AsA-GSH cycle, a supportive cycle behind the enzymatic antioxidative defence. The redox state of GSH was significantly leaning towards the oxidised form (GSSG) under the influence of 0.4 mM metazachlor at 14 DAT.

Metazachlor induces membrane lipid peroxidation and shifts in pigment and nutrient profiles

The increasing trend in TBA-reactive metabolites of 39 % and 43 % in 0.2 mM and 0.4 mM metazachlor-exposed plants respectively, indicated that cellular membranes were destabilised by lipid peroxidation at 28 DAT (Table 2). No clear shifts in pigment profile were observed 2 weeks after application. Twenty-eight DAT however, the pigment profile in *B. napus* leaves was influenced by 0.2 mM metazachlor with an increased chlorophyll concentration, due to an increment of chlorophyll *a* (Table 2). Fourteen-day-old plants exposed to 0.4 mM metazachlor contained higher nutrient levels in their aboveground areal parts. Levels of macronutrients, such as potassium, calcium and phosphorus, as well as of micronutrients, such as manganese and copper, increased significantly within a range of 25 to 80 % under the influence of 0.4 mM metazachlor (Table 1). Twenty-eight DAT, the nutrient profile in metazachlor-treated plants differed from control plants, with significant losses of phosphorus and significant augmentation of magnesium and sodium (Table 2).

DISCUSSION

In the present study, controlled growth experiments of oilseed rape were carried out using microcosms in temperature-, light- and moisture-controlled growth chambers. This experimental set-up enabled us to investigate the specific impact of metazachlor on the crop *B. napus*, with exclusion of the complex interaction with soil characteristics and soil organisms, the direction and rate of drainage and the presence of herbivores, such as snails. Hence, the underlying mechanisms that ultimately determine the degree of phytotoxicity could be studied.

The detoxification metabolism in B. napus is activated 2 to 4 weeks after metazachlor application

The detoxification capacity of a crop is crucial for the neutralisation of xenobiotic compounds and ultimately determines the potential harm induced by that compound, either in form of direct interaction or via the induction of oxidative stress. The presence of metazachlor in the aboveground organs of young oilseed seedlings pointed out that metazachlor was taken up by roots and translocated into the shoots within 2 weeks after application. The decrease of the internal metazachlor concentration in the aboveground parts of *B. napus* during the subsequent weeks indicated the activation of the detoxification metabolism (Figure 1). The rate of detoxification decreased with increasing metazachlor dose 2 weeks after application, which might indicate that the detoxification metabolism is either suppressed by the high internal metazachlor concentration or that it reached its maximal turnover (Figure 1). Taking into account the rate of detoxification, the results of this laboratory test set up suggest that metazachlor might be entirely metabolised internally within 10 to 12 weeks after application (Figure 1). This result is in line with reported half-lives of metazachlor in the soil, that range

between 19 to 82 days [37]. In general, the detoxification rate of herbicides is determined by the activity of cytochrome P450 peroxidases, GSH and GST. The detoxification of chloroacetamides does not involve phase I metabolisation by cyt P450 and is only facilitated by GST-mediated conjugation [38]. However, the tolerance of a crop towards a certain herbicide is not solely determined by the activity of GST. Glutathione concentration and redox state are also important [10]. After metazachlor application, the increased activity of GST at both time points and the increment in GSSG fraction at 14 DAT suggest that the detoxification of metazachlor was activated in oilseed rape (Figure 6). Two weeks after metazachlor application, the increased activity of GST with affinity towards CDNB and Npa substrates indicates that metazachlor and its metabolites were being conjugated with GSH prior to storage in the cell wall or in the vacuole (Figure 6). Four weeks after application, GST showed affinity to all tested GST substrates (Figure 6). Phi class GST's are closely associated with detoxification of chloroacetamides [17]. Since fluorodifen has been associated with tau-class GST activity [39] and CDNB is considered as a non-specific substrate [11], it can be considered that both tau and phi classes of GSTs, which are most important routes for detoxification in plants [40], are involved in detoxification of metazachlor. Since the glutathione redox state is promoted towards its oxidised form (GSSG) under metazachlor treatment, GSH biosynthesis might not be able to provide the demand for GSH at this time point (Table 1). Two weeks later, the augmented activity of GST indicates that glutathione is still actively consumed for metazachlor-conjugation at this time point (Table 2, Figure 6). In accordance with our results, the related chloroacetamide metolachlor induced a 5-fold increase in GST activity in maize [41]. Although Viger et al. [41] did not observe any changes in GSH content, Štajner et al. [20] noticed decreased GSH contents in lettuce, pea and bean seeds under the influence of chloroacetamides, alachlor and metolachlor.

Metazachlor-induced oxidative stress results in membrane damage of plant cells

The presence of ROS, such as H_2O_2, in leaves of metazachlor exposed seedlings could not be revealed with the 3,3'-diaminobenzidine staining technique. However, the increased activity of enzymes involved in antioxidative defence and cell wall lignification and the activation of the AsA-GSH cycle, indirectly suggest the induction of pro-oxidants under the influence of metazachlor, 2 and 4 weeks after application (Tables 1 and 2, Figure 6). The total antioxidative capacity in leaf cells, determined by the ferric reducing antioxidative capacity (FRAP), comprises both water-soluble antioxidants, such as GSH, AsA, proline, phenolic compounds, membrane-bound molecules, and water-insoluble antioxidants, such as carotenoids and tocopherols (vitamin E) [42]. The increase of the lipophilic fraction of antioxidants and the increase of carotenoid concentration at 28 DAT (Table 2), suggest a potential role for tocopherols as antioxidative compounds at this time point. Tocopherols have a significant role in herbicide-induced oxidative stress because of their ability to protect membrane-localised polyunsaturated fatty acids against ROS-induced lipid peroxidation [43,44]. However, the simultaneous increase in lipid peroxidation suggests insufficient protection of leaf tissue against oxidative stress. Membrane integrity was estimated via potassium leakage and lipid peroxidation. The latter was significantly induced by metazachlor at 28 DAT (Table 2). Whereas the destabilisation of membranes can directly be induced through the inhibition of fatty acid biosynthesis by metazachlor, this also can be the result of metazachlor-induced oxidative stress. That these responses in membrane destabilisation became significant after 4 weeks could either be explained by the fact that the inhibition of VLCFA is a relatively slow process [23] or the fact that oxidative damage is a secondary side-effect of metazachlor. In general, herbicide-induced oxidative stress has been described in several crops [18,19] and in particular also for chloroacetamides, such as alachlor and metolachlor [20,21]. The induction of the antioxidative enzymes SOD, APX, CAT and GR at

2 and 4 weeks after metazachlor application indicated metazachlor-induced oxidative stress (Tables 1 and 2). The reduced CAT activity in the highest metazachlor treatment at 14 DAT could be linked to the high phytotoxic effects of metazachlor. However, the high sensitivity of CAT towards high levels of H_2O_2 has been described in different crop species under influence of various stresses, such as copper [45], herbicides [46] and high and low temperatures [47]. The high activities of cell wall bound peroxidases that use syringaldazine and guaiacol as substrates (Tables 1 and 2) and that are involved in lignin biosynthesis, suggest either the apoplastic presence of ROS or the activation of cell wall lignification [48,49]. Increased cell wall lignification could result in a reduced permeability by the establishment of a physical barrier and can therefore allow the cell to better protect itself against xenobiotics. Lignin is known to be responsive to a range of stresses. Biotic and abiotic stresses (such as metals), are known to induce lignification in the walls of cells that do not lignify under non-stress responses [50], however this has not been described yet for herbicides. The increased activity of ascorbate peroxidase (APx) under the influence of 0.2 mM metazachlor at 14 DAT indicates that H_2O_2 is being converted actively into water and oxygen (Figure 6) and suggests the activation of the AsA-GSH cycle. This assumption is supported by the significant shift of the glutathione redox state towards its oxidised form, glutathione disulphide (GSSG), at 14 DAT and the increased activity of GR at 28 DAT under the influence of metazachlor (Figure 6). Together with glutathione's shift towards it's oxidised form, the increased activity of GST implies that GSH is consumed in the detoxification metabolism of metazachlor. Therefore, it can be presumed that GSH fulfils a dual role in both antioxidative defence and detoxification (Figure 6). Although ROS are known to induce oxidative damage, they also have an important function in signalling [51]. Hydrogen peroxide has been shown to regulate GST in vivo [52] and can therefore influence the rate of detoxification. GST induction by ROS would appear to represent an adaptive response as these enzymes detoxify some of the toxic carbonyl-,

peroxide-, and epoxide-containing metabolites produced within the cell by oxidative stress [53].

Metazachlor inhibits growth, induces fasciation and causes membrane peroxidation on the short term

Phytotoxic effects of metazachlor on oilseed rape became apparent shortly after its application, with a reduction of germination (data not shown), the manifestation of fasciation (Figure 2) and the occurrence of mortality (data not shown). Fasciation of the leaves was already induced immediately after seedling emergence (Figure 2). Typical symptoms of chloroacetamide herbicides, such as stunted growth, cupped and wrinkled leaves, shortened main veins and leaf fasciation were induced and were formerly observed in *Arabidopsis thaliana* exposed to related chloroacetamides, acetolachlor, alachlor and metolachlor [5]. Metazachlor-induced fasciation could be attributed to the mode of action of chloroacetamides, whereby inhibition of VLCFA synthesis has led to the inhibition of normal cell division [54,55]. During the further development of the crop, stem and shoot weight of the emerged seedlings was suppressed by metazachlor (Figure 3A-C, Table 1 and 2). Reductions in crop shoot length have previously been observed in *Sorghum sp*. under the influence of the chloroacetamide, metolachlor [56]. Although the timing of appearance of the leaves of *B. napus* seedlings seemed not to be influenced by metazachlor (Figure 5), the surface of the leaves and the petiole length were noticeably reduced (Supplemental data S1) and could be linked with an insufficient capacity of light capitation for photosynthesis and therefore reduced shoot weight. However, the pigment profile was not influenced as such (Tables 1 and 2). In contrast to previous studies where pigment content was negatively affected by pesticides [8,57], chlorophyll and carotenoid concentrations rather tended to increase under the influence of metazachlor (Tables 1 and 2). Although, metazachlor did not have any effect

on the rate of leaf development up to 5 weeks after treatment, metazachlor-exposed plants tended to develop leaves faster than control plants between 5 and 7 weeks after treatment (Figure 5). Taking into consideration the development of leaves and the similar weights of metazachlor exposed and non-exposed seedlings 9 weeks after application (Figure 3C), the seedlings appeared to recover from the initial herbicide stress by investing in leaf development.

Conclusions

In conclusion, this controlled microcosm experiment demonstrated that, on the short term, metazachlor induces significant adverse effects on oilseed rape at morphological level. Together with an induction of the detoxification metabolism and the activation of the antioxidative defence responses, a reduction in growth investment was observed. These observations underpin the hypothesis that plants are investing energy in detoxification of the absorbed metazachlor and in the neutralisation of metazachlor-induced ROS, over shoot growth. This strategy seems to suffice for the plants to recover, as 9 weeks after application their weight did not differ any more from the non-treated plants. When considering the weight of the aboveground areal plant parts, the metazachlor-exposed plants appear to be able to recover from the initial chemical-induced stress.

ACKNOWLEDGEMENT

We thank A. Wijgaerts and C. Put for their technical assistance of the microcosm experiment. The present study was supported by a PhD grant for Hanne Vercampt from the Institute for the Promotion of Innovation through Science and Technology in Flanders (IWT-Vlaanderen). We especially thank G. Chotoklieva for the technical assistance of the metazachlor analyses.

REFERENCES

1. Fuerst EP. 1987. Understanding the mode of action of the chloroacetamide and thiocarbamate herbicides. *Weed Technol.* 1:270–277.

2. Mamy L, Barriuso E, Gabrielle B. 2005. Environmental fate of herbicides trifluralin, metazachlor, metamitron and sulcotrione compared with that of glyphosate, a substitute broad spectrum herbicide for different glyphosate-resistant crops. *Pest Manag. Sci.* 61:905–916.

3. Carpenter D, Boutin C. 2010. Sublethal effects of the herbicide glufosinate ammonium on crops and wild plants: Short-term effects compared to vegetative recovery and plant reproduction. *Ecotoxicology*. 19:1322–1336.

4. Foy CL, Witt HL. 1990. Seed Protectants Safen Sorghum (Sorghum bicolor) Against Chloroacetamide Herbicide Injury. 4:886–891.

5. DeRidder BP, Goldsbrough PB. 2006. Organ-specific expression of glutathione S-transferases and the efficacy of herbicide safeners in Arabidopsis. *Plant Physiol.* 140:167–175.

6. Cui J, Zhang R, Wu GL, Zhu HM, Yang H. 2010. Salicylic acid reduces Napropamide toxicity by preventing its accumulation in rapeseed (Brassica napus L.). *Arch. Environ. Contam. Toxicol.* 59:100–108.

7. Jiang L, Ma L, Sui Y, Han SQ, Wu ZY, Feng YX, Yang H. 2010. Effect of manure compost on the herbicide prometryne bioavailability to wheat plants. *J. Hazard. Mater.* 184:337–344.

8. Xiao LY, Jiang L, Ning HS, Yang H. 2008. Toxic reactivity of wheat (Triticum aestivum) plants to herbicide isoproturon. *J. Agric. Food Chem.* 56:4825–4831.

9. Jablonkai I, Biology M, Stress P, Pathology P, Science W, April R, Sc A, Sc A, Gst S, Gstcacetofhlor R, Re- P. 1991. Role of Glutathione and Glutathione S-Transferase in the Selectivity of Acetochlor in Maize and Wheat. 231:221–231.

10. Hatton PJ, Dixon D, Coleb DJ, Edwardsa R. 1996. Glutathione Transferase Activities and Herbicide Selectivity in Maize and Associated Weed Species. *Pestici. Sci.* doi:10.1002/(SICI)1096-9063(199603)46:3<267::AID-PS347>3.0.CO;2-N.

11. Cole DJ. 1994. Detoxification and activation of agrochemicals in plants. *Pestic. Sci.* 42:209–222.

12. Scarponi L, Quagliarini E, Del Buono D. 2006. Induction of wheat and maize glutathione S-transferase by some herbicide safeners and their effect on enzyme activity against butachlor and terbuthylazine. *Pest Manag. Sci.* 62:927–932.

13. Dixon DP, Edwards R. 2010. Glutathione Transferases. *Arab. B.*, pp 1–15. doi:e0131. 10.1199/tab.0131.

14. Dixon DP, Cummins I, Cole DJ, Edwards R. 1998. Glutathione-mediated detoxification systems in plants. *Curr. Opin. Plant Biol.* 1:258:266.

15. Edwards R, Dixon DP, Walbot V. 2000. Plant glutathione S -transferases: enzymes with multiple functions in sickness and in health. 5:193–198.

16. Marrs K a. 1996. the Functions and Regulation of Glutathione S-Transferases in Plants. *Annu. Rev. Plant Physiol. Plant Mol. Biol.* 47:127–158.

17. Cho HY, Yoo SY, Kong KH. 2006. Cloning of a rice tau class GST isozyme and characterization of its substrate specificity. *Pestic. Biochem. Physiol.* 86:110–115.

18. Gill SS, Tuteja N. 2010. Reactive oxygen species and antioxidant machinery in abiotic stress tolerance in crop plants. *Plant Physiol. Biochem.* 48:909–930.

19. Faheed FA. 2012. Comparative effects of four herbicides on physiological aspects in Triticum sativum L. *Afr. J. Ecol.* 50:29–42.

20. Štajner D, Popović M, Štajner M. 2003. Herbicide induced oxidative stress in lettuce, beans, pea seeds and leaves. *Biol. Plant.* 47:575–579.

21. Liu HJ, Xiong MY, Tian BL. 2012. Comparative phytotoxicity of Rac-metolachlor and S-metolachlor on rice seedlings. *J. Environ. Sci. Heal. Part B.* 47:410–419.

22. Dean J V, Gronwald JW, Eberlein C V. 1990. Induction of glutathione s-transferase isozymes in sorghum by herbicide antidotes. *Plant Physiol.* 92:467–73.

23. Dayan FE, Watson SB. 2011. Plant cell membrane as a marker for light-dependent and light-independent herbicide mechanisms of action. *Pestic. Biochem. Physiol.* 101:182–190.

24. Kopsell D a., Armel GR, Abney KR, Vargas JJ, Brosnan JT, Kopsell DE. 2011. Leaf tissue pigments and chlorophyll fluorescence parameters vary among sweet corn genotypes of differential herbicide sensitivity. *Pestic. Biochem. Physiol.* 99:194–199.

25. Lancashire PD, Bleiholder H, Boom T Van Den, LangelÜDdeke P, Stauss R, Weber E, Witzenberger a. 1991. A uniform decimal code for growth stages of crops and weeds. *Ann. Appl. Biol.* 119:561–601.

26. Dhindsa R, Plumbdhinsa P, Thorpe T. 1981. Leaf senescence: correlated with increased levels of membrane permeability and lipid peroxidation, and decreased levels of superoxide dismutase. *J. Exp. Bot.* 32:93–101.

27. Lichtenthaler HK, Buschmann C, Knapp M. 2005. How to correctly determine the different chlorophyll fluorescence parameters and the chlorophyll fluorescence decrease ratio RFd of leaves with the PAM fluorometer. *Photosynthetica*. 43:379–393.

28. Daudi A, Cheng Z, O'Brien JA, Mammarella N, Khan S, Ausubel FM, Bolwell GP. 2012. The Apoplastic Oxidative Burst Peroxidase in *Arabidopsis* Is a Major Component of Pattern-Triggered Immunity. *Plant Cell*. 24:275–287.

29. Kerchev P, Ivanov S. 2008. Influence of extraction techniques and solvents on the antioxidant capacity of plant material. *Biotechnol. Biotechnol. Equip.* 22:556–559.

30. McCord JM, Fridovich I. 1969. Superoxide dismutase: an enzymatic function for erythrocuprein (hemocuprein). *J. Biol. Chem.*:6049–6055.

31. Bergmeyer HU, Gawenn K, Grassl M. 1974. Enzymes as biochemical reagents. *Methods Enzym. Anal.*, pp 425–522.

32. Czaninski Y, Imberty A, Catesson A. 1984. Cytochemical-localization and parallel biochemical analysis of vegetal peroxidases. *Biol. Cell*. 51:A34–A34.

33. Schröder P, Collins C. 2002. Conjugating Enzymes Involved in Xenobiotic Metabolism of Organic Xenobiotics in Plants. *Int. J. Phytoremediation*. 4:247–265.

34. Scalla R, Roulet A. 2002. Cloning and characterization of a glutathione S-transferase induced by a herbicide safener in barley (Hordeum vulgare). *Physiol. Plant.* 116:336–344.

35. Gerbling K, Kelly G, Fischer K, Latzko E. 1984. Partial purification and properties of soluble ascorbate peroxidases from pea leaves. *J. Plant Physiol.* 115:59–67.

36. Queval G, Noctor G. 2007. A plate reader method for the measurement of NAD, NADP, glutathione, and ascorbate in tissue extracts: Application to redox profiling during Arabidopsis rosette development. *Anal. Biochem.* 363:58–69.

37. Mamy L, Gabrielle B, Barriuso E. 2008. Measurement and modelling of glyphosate fate compared with that of herbicides replaced as a result of the introduction of

glyphosate-resistant oilseed rape. *Pest Manag. Sci.*:262–275. doi:10.1002/ps.1519.

38. Coleman JOD, Randall R, Blake-Kalff MMA. 1997. Detoxification of xenobiotics in plant cells by glutathione conjugation and vacuolar compartmentalization: A fluorescent assay using monochlorobimane. *Plant, Cell Environ.* 20:449–460.

39. Jo HJ, Lee JJ, Kong KH. 2011. A plant-specific tau class glutathione S-transferase from Oryza sativa with very high activity against 1-chloro-2,4-dinitrobenzene and chloroacetanilide herbicides. *Pestic. Biochem. Physiol.* 101:265–269.

40. Thom R, Cummins I, Dixon DP, Edwards R, Cole DJ, Lapthorn AJ. 2002. Structure of a tau class glutathione S-transferase from wheat active in herbicide detoxification. *Biochemistry*. 41:7008–7020.

41. Viger PR, Eberlein C V, Fuerst EP, Gronwald JW. 1991. Effects of CGA-154281 and temperature on metolachlor absorption and metabolism , glutathione content , and glutathione-s-transferase activity in corn. *Weed Sci.* 39:324–328.

42. Prior R, Wu X, Schaich K. 2005. Standarized Methods for the Determination of Antioxidant Capacity and Phenolics in Foods and Dietary Supplements. *J. Agric. Food Chem.* 53:4290–4302.

43. Fryer MJ. 1992. The antioxidant effects of thylakoid Vitamin E (alpha-tocopherol). *Plant, Cell Environ.* 15:381–392.

44. Munné-Bosch S. 2005. The role of α-tocopherol in plant stress tolerance. *J. Plant Physiol.* 162:743–748.

45. Luna CM, Gonzalez CA, Trippi VS. 1994. Oxidative damage caused by an excess of copper in Oat leaves. *Plant Cell Physiol.*:11–15.

46. Song NH, Yin X Le, Chen GF, Yang H. 2007. Biological responses of wheat (Triticum

aestivum) plants to the herbicide chlorotoluron in soils. *Chemosphere*. 68:1779–1787.

47. Feierabend J, Schaan C, Hertwig B. 1992. Photoinactivation of Catalase Occurs under Both High- and Low-Temperature Stress Conditions and Accompanies Photoinhibition of Photosystem II. *Plant Physiol.* 100:1554–1561.

48. Bestwick CS. 1998. Localized Changes in Peroxidase Activity Accompany Hydrogen Peroxide Generation during the Development of a Nonhost Hypersensitive Reaction in Lettuce. *Plant Physiol.* 118:1067–1078.

49. Lee BR, Kim KY, Jung WJ, Avice JC, Ourry A, Kim TH. 2007. Peroxidases and lignification in relation to the intensity of water-deficit stress in white clover (Trifolium repens L.). *J. Exp. Bot.* 58:1271–1279.

50. Wang S, Li H, Lin C. 2013. Physiological, biochemical and growth responses of Italian ryegrass to butachlor exposure. *Pestic. Biochem. Physiol.* 106:21–27.

51. Mittler R, Vanderauwera S, Gollery M, Van Breusegem F. 2004. Reactive oxygen gene network of plants. *Trends Plant Sci.* 9:490–498.

52. Levine A, Tenhaken R, Dixon R, Lamb C. 1994. H2O2 from the oxidative burst orchestrates the plant hypersensitive disease resistance response. *Cell*. 79:583–593.

53. Hayes JD, Pulford DJ. 1995. The Glutathione S-Transferase Supergene Family: Regulation of GST* and the Contribution of the lsoenzymes to Cancer Chemoprotection and Drug Resistance. *Crit. Rev. Biochem. Mol. Biol.* 30:445–600.

54. Böger P, Matthes B, Schmalfuß J. 2000. Towards the primary target of chloroacetamides –new findings pave the way. *Pest Manag. Sci.* 56:497–508.

55. Wu J, Hwang I-T, Hatzios KK. 2000. Effects of Chloroacetanilide Herbicides on Membrane Fatty Acid Desaturation and Lipid Composition in Rice, Maize, and

642 Sorghum,. *Pestic. Biochem. Physiol.* 66:161–169.

643 56. Wilkinson RE, Duncan RR, Meredith SA, Hatzios KK. 1993. Growth and
644 physiological responses of sorghum cultivars exposed to excess H + and the herbicide
645 metolachlor. *Can. J. Bot.*:533–540.

646 57. Serra AA, Couée I, Renault D, Gouesbet G, Sulmon C. 2015. Metabolic profiling of
647 Lolium perenne shows functional integration of metabolic responses to diverse
648 subtoxic conditions of chemical stress. *J. Exp. Bot.* 66:1801–1816.

649

FIGURE LEGENDS

Figure 1. Metazachlor concentration in aboveground plant parts of *B. napus* 14, 28 and 42 DAT with 0 mM, 0.2 mM and 0.4 mM metazachlor. Data are presented as average values of minimal 3 biological replicates ± SE.

Figure 2. Detailed images of *B. napus* exposed to 0 mM, 0.2 mM and 0.4 mM metazachlor at 21 DAT. Plants exposed to 0.2 mM and 0.4 mM metazachlor displayed malformations of the leaves.

Figure 3. Aboveground fresh weight of *B. napus* 14 DAT (A), 28 DAT (B) and 63 DAT (C) with 0 mM, 0.2 mM and 0.4 mM metazachlor. Data are presented as average values of minimal 10 biological replicates ± SE. (*post-hoc values: $p < 0.05$)

Figure 3. Overview images of *B. napus* exposed to 0 mM, 0.2 mM and 0.4 mM metazachlor at 14, 28 and 42 DAT.

Figure 4. Emergence and leaf development of *B. napus* over time, treated with (A) 0 mM, (B) 0.2 mM and (C) 0.4 mM metazachlor, expressed as the amount (%) of all measured plants that are situated in a specific developmental stage at a certain time point (DAT). Different growth stages are depicted as described by Lancashire et al. 1991.

Figure 5: An overview of the relative enzyme activities and metabolite concentrations that play a role in either the detoxification of herbicides or the antioxidant defence mechanism. Data are expressed relative to control values (dashed line). Abbreviations used: APx

(ascorbate peroxidase), AsA (ascorbate), CDNB (chlorodinitrobenzene), GST (glutathione-S-transferase), DHA (dehydroascorbate), GSSG (glutathione disulphide), GSH (glutathione), GR (glutathione reductase), Npa (nitrophenylacetate), NADPH (Nicotinamide adenine dinucleotide phosphate). (* post-hoc value $p < 0.05$)

678 **SUPPLEMENTAL DATA**

679 **Supplemental data S1.** Leaf development of *B. napus* monitored weekly, after pre-emergent
680 application with 0 mM (dotted line), 0.2 mM (dashed line) and 0.4 mM (solid line)
681 metazachlor. Leaf surface (A) area and petiole length (B) were measured at 12, 19, 26 and 33
682 DAT.

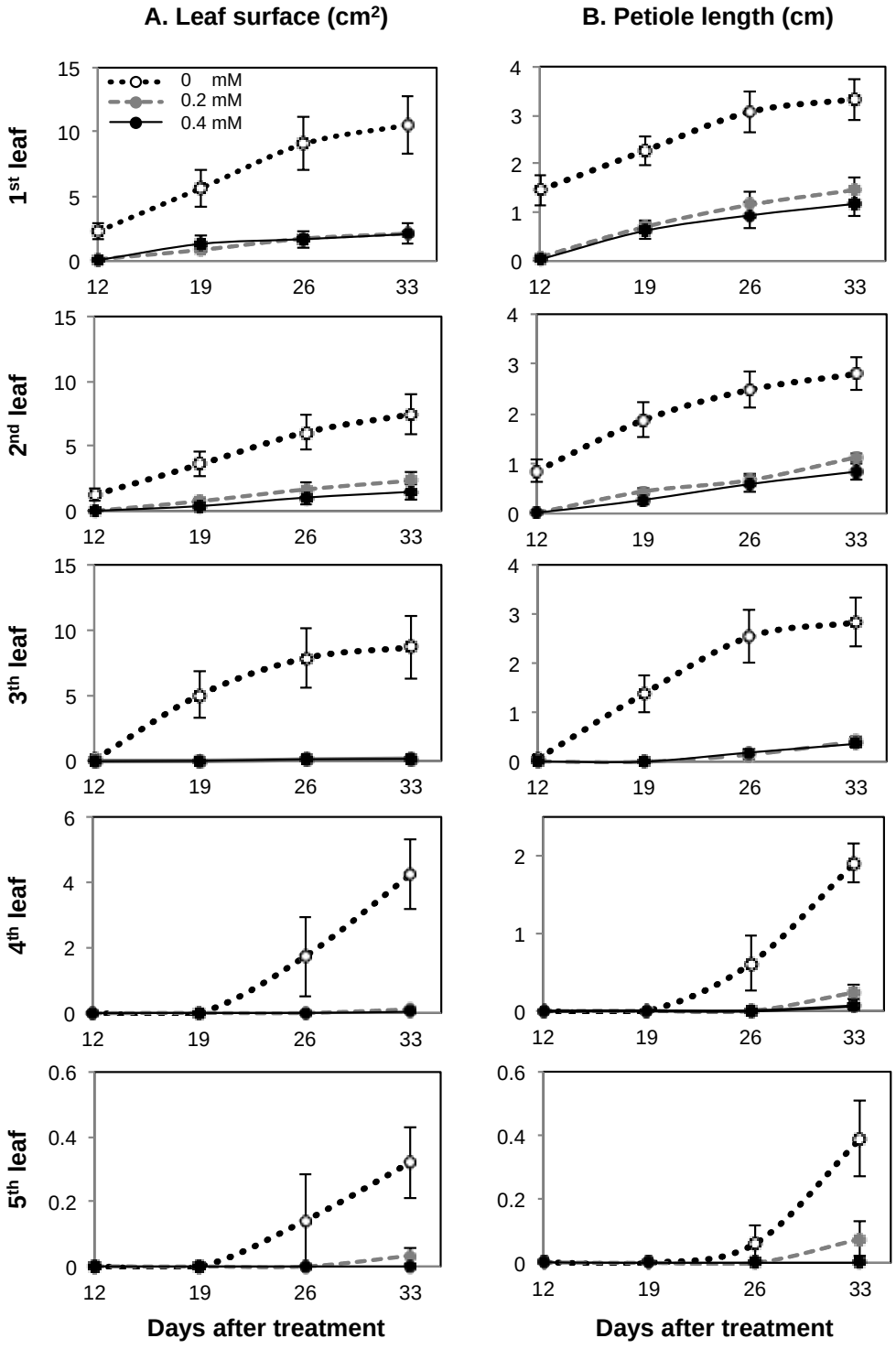

683

Supplemental data S2. Qualitative determination of H_2O_2 in leaves of *B. napus*, 14 days after metazachlor application (0 mM, 0.2 mM, 0.4 mM) by 3,3'-diaminobenzidine staining. Three biological replicates are shown per treatment.